

Assessment of Atrial Septal Defect Area Changes During Cardiac Cycle by Live Three-Dimensional Echocardiography

Ming-Xing XIE, MD
Ling-Yun FANG, MD
Xin-Fang WANG, MD
Qing LU, MD
Xiao-Fang LU, MD
Ya-Li YANG, MD
Jing WANG, MD
Lin HE, MD
Zhao-Xiao PU, MD
Ling LI, MD

Abstract

Objectives. To investigate the accuracy of measurement of the atrial septal defect (ASD) area and dynamic change by live three-dimensional echocardiography (L3DE).

Methods. L3DE was performed in patients with ASD using a three-dimensional workstation to obtain the en face view of the ASD and measure its area at the peak of P-wave, the peak of R-wave, the initial and the destination point of T-wave, and the period of P-T. Parameters derived from L3DE were compared with intraoperative measurements.

Results. The ASD area changed significantly during cardiac cycles (mean change 46.1%, $p < 0.0001$; range 15.2 - 72.5%), with the maximal area at endsystole and the minimal area at enddiastole. There was excellent correlation between L3DE and intraoperative measurements for the area of ASD at the peak of P-wave ($r = 0.92$). There were good correlations between the two methods during the other phases of cardiac cycle ($r = 0.81 - 0.86$).

Conclusions. L3DE provides accurate and feasible measurements of the ASD area. Investigation of the dynamic changes during the cardiac cycle may lead to an improved understanding of the hemodynamics of ASD.

J Cardiol 2006 Apr; 47(4): 181 - 187

Key Words

■ Echocardiography (live three-dimension) ■ Hemodynamics
■ Congenital heart disease (atrial septal defect)

INTRODUCTION

Atrial septal defect (ASD) accounts for approximately 10 - 15% of all cases of congenital heart malformation and is the most common lesion in

adult congenital cardiac disease¹). Recently, the development of new techniques such as minimal access surgery and transcatheter occlusion has made it more difficult to decide on the most appropriate treatment for any particular patient²⁻⁴).

Department of Echocardiography, Union Hospital, Tongji Medical College, Huazhong University of Science and Technology, Wuhan, China

Address for correspondence: Ming-Xing XIE, MD, Department of Echocardiography, Union Hospital, Tongji Medical College, Huazhong University of Science and Technology, 1277 Jiefang Avenue, Wuhan, 430022, PR China; E-mail: xiexm64@126.com

Manuscript received November 4, 2005; revised December 19, 2005; accepted January 4, 2006

Precise information about the defect area and its shape is desirable for the selection of patients for interventions and the choice of device size for transcatheter closure⁵).

At present, there is no imaging technique which can display the en face view of ASD directly. However, live three-dimensional echocardiography (L3DE) can reveal the three-dimensional relationships between the anatomical structures of the heart and dynamic changes during the cardiac cycle⁶). Therefore, the present study had to determine the area of ASD by L3DE, for comparison with areas obtained by intraoperative measurements. Moreover, dynamic changes of the ASD areas during selected phases of the cardiac cycle were evaluated, to improve the understanding of the hemodynamics of ASD.

SUBJECTS AND METHODS

Patient population

The study population consisted of 31 consecutive patients (13 males and 18 females) aged 2 to 47 years (mean age 23.6 ± 16.1 years) with ASD referred for surgery. Twenty-five patients had secondary ASD and six patients had primary ASD. All patients had New York Heart Association (NYHA) functional classification I - II grade and were in sinus rhythm.

Live three-dimensional data acquisition

All patients underwent L3DE using Philips Sonos 7500 hardware (Philips Medical Systems), which has the capacity for obtaining full volume acquisitions of three-dimensional datasets by a matrix array transducer with a frequency of 2 - 4 MHz. The patient was kept in the supine or left lateral semidecubitus position, with the electrocardiography electrodes connected to confirm the timing of the cardiac cycle. First, the two-dimensional image with apical four-chamber view was displayed in the middle of the monitor, using the method of biplane vertical crossing to define the scope. Second, full volume acquisition was utilized to generate a volume rendering dataset. Volumetric images were acquired and stored in the hard disk. After the procedure, the dataset was copied to the optical disk for analysis.

Area measurements

The stored dataset in the optical disk was transferred to a computer (Echo-scan, version 4D Cardio

View RT 1.2, Tom Tec Imaging System, Inc). The whole dataset was cropped appropriately in three mutual perpendicular reference planes, the coronal plane, sagittal plane and transverse plane, to display the apical four-chamber view, apical two-chamber view and short-axis view simultaneously, adjusting the interatrial septa to parallel to the reference plane midline. Then the whole view (en face view) of the interatrial septa was obtained from the right atrium. The cardiac cycle phases at the peak of P-wave, the peak of R-wave, the initial and the destination point of T-wave, and the period of P-T were defined by electrocardiography, and the outline of the ASD area was drawn accordingly.

The percentage change in the area and length of each measurement during the cardiac cycle were then calculated using the following formula: % change during the cardiac cycle = $(\text{largest measurement} - \text{smallest measurement}) / \text{largest measurement} \times 100\%$.

All patients underwent surgery with extracorporeal circulation. With the heart in diastolic arrest, the area of the defect before repair was calculated from the lengths of the major (a) and the minor (b) axis, using the formula: area of the defect = $1/4 ab$ ^{7,8}).

Statistical analysis

Differences between the measurements were compared by the paired t -test. Statistical correlations between the two measurements were tested by simple linear correlation. Data are presented as mean \pm SD. A value of $p < 0.05$ was considered statistically significant. Agreement between L3DE and surgery was evaluated using the Bland and Altman graph⁹).

Interobserver and intraobserver variability

Ten randomly selected patients underwent L3DE. The ASD areas were measured by two examiners on two separate occasions and a third time by one observer. Interobserver and intraobserver variability was defined as the difference between two measurements, expressed as the percentage of the mean of two values and the standard deviation of the difference of the two values. Interobserver and intraobserver variabilities were $2.5 \pm 7.2\%$ and $1.3 \pm 9.0\%$ respectively.

RESULTS

Defect area measurements

High-quality L3DE images were obtained (Fig. 1) and the ASD area could be measured by the Tom Tec Imaging System in all 31 patients (Fig. 2). The ASD area changed during cardiac cycle, with the maximal area at endsystole and the minimal area at enddiastole. Fig. 3 describes the area change during one cardiac cycle in all patients expressed as the mean area of the selected phase. The ASD area decreased gradually with atrial contraction. At the beginning of P-wave, the minimal area was reached at enddiastole which was the peak of R-wave. The ASD area increased gradually during ventricular contraction and the maximal area was reached at endsystole, which was the destination point of T-wave. The ASD areas changed significantly during the cardiac cycle from 14.3 ± 1.2 to $8.9 \pm 0.6 \text{ cm}^2$ ($p < 0.0001$). The percentage change ranged from 15.2% to 72.5%, with a mean of 46.1%.

Comparison of live three-dimensional echocardiography and intraoperative measurements

Mean area measured by intraoperative assessment was $4.34 \pm 2.31 \text{ cm}^2$. There was an excellent correlation between the measurements by L3DE at the peak of P-wave and intraoperative measurements ($y = 0.94x + 0.53$; $r = 0.92$, $p < 0.0001$). The mean difference between the average values of ASD area obtained by the two methods was $0.28 \pm 0.85 \text{ cm}^2$ (Fig. 4). There were also good correlations in the other phases of cardiac cycle, including at the peak of R-wave, the initial and the destination point of T-wave, and the period of P-T. The correlation coefficients were 0.84, 0.86, 0.81 and 0.86 respectively.

DISCUSSION

Two-dimensional echocardiography and color Doppler imaging are the noninvasive procedures most widely used for the detection of ASD¹⁰. However, only the planar structure of the heart is imaged and the ASD diameter in two dimensional section is obtained. The whole defect cannot be displayed in three-dimensional view and measurement of the ASD area is impossible. L3DE is now available for clinical application¹¹⁻¹³. The technique utilizes a matrix transducer which offers steering in both the elevation and the azimuth planes, thus permitting instantaneous volume scan. Moreover, the

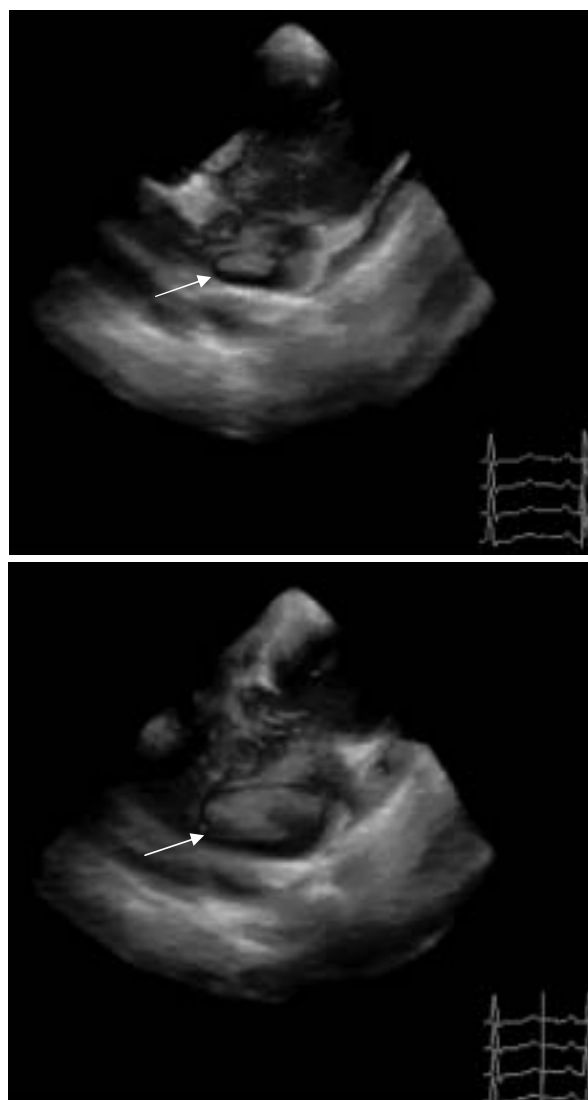


Fig. 1 Three-dimensional images of atrial septal defects viewed from the right atrium

Upper: Enddiastole (at the peak of R-wave) stop frame images with the minimal defect area and an ellipse shape (arrow).

Lower: Endsystole (at the destination point of T-wave) stop frame images with the maximal defect area (arrow).

new matrix array probe used 16: 1 parallel processes to scan a pyramidal volume which corresponds to the two-dimensional scanning line density, so can provide dynamic imaging of entire cardiac structures in bigger volume¹⁴. For this reason, the acquisition and instantaneous display of the ASD area is possible from live three-dimensional images and the full volume dataset is easily and rapidly obtained.

ASD area is the main index for the quantitative analysis of ASD. The quantity of ASD shunt flow

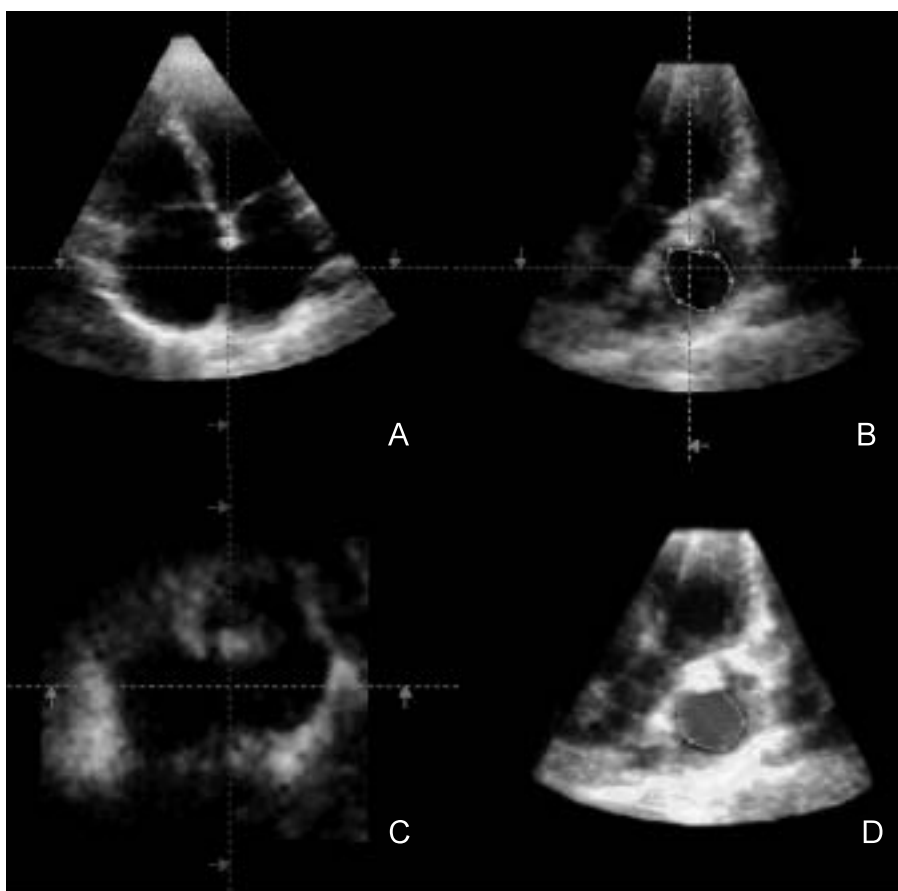


Fig. 2 Measurement of atrial septal defect area from Tom Tec workstation

A, B, C: Three mutual perpendicular reference planes of two-dimensional echocardiograms displaying the defect simultaneously.

D: Defect area is manually outlined along the borderline of the defect from the three-dimensional dataset.

is determined by the ASD area and shunt velocity¹⁵). The differential pressure which controls the shunt velocity between the cardiac atria is minimal, and generally speaking, this value is 3 - 5 mmHg. Therefore, the shunt velocity of ASD flow is low and shunt flow is mainly determined by the ASD area. Accordingly, the ASD area was measured and dynamic changes during cardiac cycle were displayed by the L3DE technique, to improve understanding and verify the hemodynamic changes caused by ASD.

In the present study, the ASD area changed significantly during the cardiac cycle. ASD area decreased gradually with atrial contraction and the minimum area was reached at enddiastole, then increased gradually during ventricular contraction and the maximum area was reached at endsystole. The dynamic changes of ASD area were related with the hemodynamics of transatrial shunting. The

pressure gradient between the atria was maximum at ventricular endsystole while shunt flow was maximum. For this reason, ASD area increased. Likewise, at ventricular enddiastole, the differential pressure between the cardiac atria and shunt flow decreased, so ASD area decreased. In addition, the dynamic changes were also related to translation of the ventricular wall. ASD area was increased during systole by the apical translation of the atrioventricular plane and decreased during diastole by the basal translation of the mitral and tricuspid annulus, which was enhanced by atrial contraction in late diastole¹⁶). Comparison of the ASD area from L3DE data in the selected phases of cardiac cycle revealed a good correlation with intraoperative measurements ($r = 0.81 - 0.92$).

Recently, transcatheter closure of ASD has become an alternative treatment approach in selected patients¹⁷). Measurement of the ASD size is one

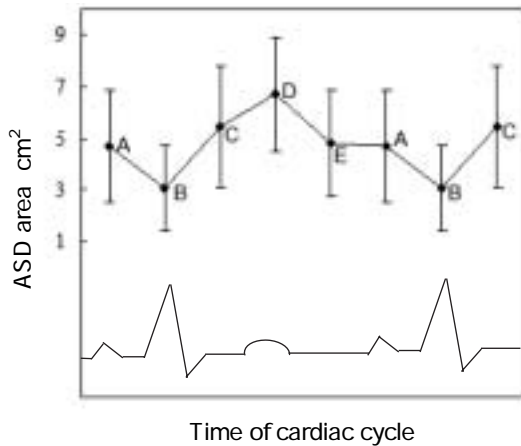


Fig. 3 Changes in the atrial septal defect area during the cardiac cycle

A, B, C, D and E are means of the atrial septal defect area at different selected times which correspond to the peak of P-wave, the peak of R-wave, the initial and the destination point of T-wave, and the period of P-T. The error bar shows the mean \pm SD respectively. ASD = atrial septal defect.

of the major factors for selection of the appropriate device. Therefore, the standard clinical technique for measurement of the maximal ASD diameter at present remains the stretched diameter measured by balloon catheterization¹⁸). The practice of this technique is limited by its disadvantages which include invasiveness, radiation exposure, and possible over-estimation because of stretching and tangential or oblique passage of the balloon through the ASD¹⁹).

The L3DE technique can measure ASD area accurately and easily, which is important to choose the most suitable device²⁰). ASD size is the only parameter to determine successful of interventional therapy when other anatomical features are suitable²¹). ASD maximum area from L3DE data is important for the planning of interventional closure and cannot always be reliably measured by two-dimensional echocardiography, which may lead to underestimation and result in residual shunt flow after device implantation¹⁶). Most importantly, the L3DE technique allows measurement of ASD area in different phases of the cardiac cycle, so determining the maximum area which may be sufficient for deciding the appropriate size of the ASD closure device and may help to avoid misplacement of devices. Further development and extensive application of L3DE may be beneficial for interventional therapy and real-time monitoring closure procedures.

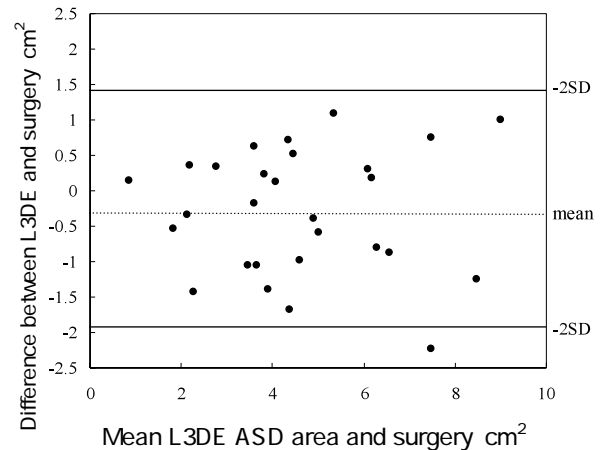
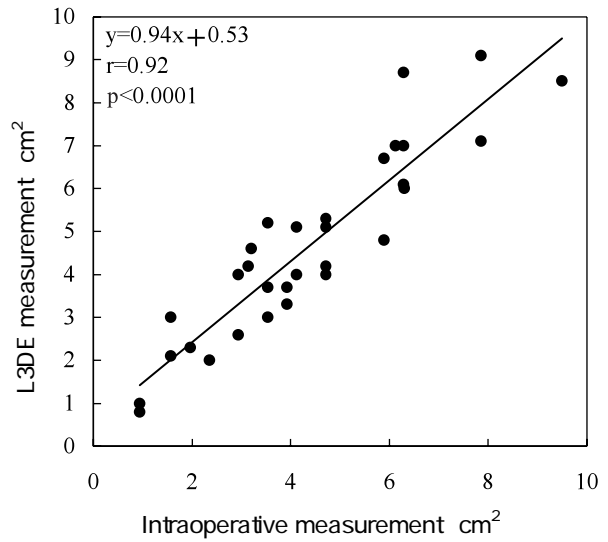


Fig. 4 Relationships between live three-dimensional echocardiographic and intraoperative measurements of the defect area measured in 31 patients

Upper: Linear regression of atrial septal defect area measured at the peak of P-wave by live three-dimensional echocardiography versus intraoperative method.

Lower: Bland-Altman graph showing differences in each pair of measurements of the defect area obtained with the two methods.

L3DE = live three-dimensional echocardiography. Other abbreviation as in Fig. 3.

There was an excellent correlation between the measurements by L3DE at the peak of P-wave and intraoperative measurements with no statistically significant difference. The reason is that intraoperative measurement was obtained in cardiac diastole and the heart was arrested in this phase²²), because extracorporeal circulation with no blood circulation in the heart resulted in relaxation of the interatrial septum. These results showed the ASD area measured by L3DE has good accuracy. Measurement at

the peak of P-wave had a better correlation coefficient than other phases of the cardiac cycle and close agreement between the two methods.

The L3DE volumetric dataset contains some motion or respiration artifacts. In addition, the intraoperative defect area was calculated assuming an ellipsoidal shape, because it was difficult to measure directly. Therefore, in agreement with other studies^{7,8}, we assumed most ASDs were ellipsoidal shape and we used only directly measured major and minor axes. Another limitation of the present study is that the ASD area measured by L3DE was obtained by off-line three-dimensional imaging. In the future, improvements of L3DE may overcome these limitations.

CONCLUSIONS

The L3DE technique can provide new information on the dynamic change of the ASD area, which can improve understanding of the hemodynamics of ASD. This information could not be obtained by conventional cross-sectional echocardiography. The technique can display stereoscopic views and complicated spatial relationships of the cardiac structures, as well as the en face view of the interatrial septum, which contributes to surgical planning. The ASD area can be measured by L3DE, which is important to choose the most suitable device in interventional therapy. L3DE may become clinically important in the diagnosis and management of ASD in the near future.

References

- 1) Li ZA, Wang XF, Yang Y: Atrial septal defect. *in* Textbook of Echocardiography (ed by Wang XF), 3rd Ed. People's Medical Publishing House, Beijing, 1999; pp 629 - 649 (in Chinese)
- 2) Burke RP, Michielon G, Wernovsky G: Video-assisted cardioscopy in congenital heart operations. *Ann Thorac Surg* 1994; **58**: 864 - 868
- 3) Sharafuddin MJ, Gu X, Titus JL, Urness M, Cervera-Ceballos JJ, Amplatz K: Transvenous closure of secundum atrial septal defects: Preliminary results with a new self-expanding nitinol prosthesis in a swine model. *Circulation* 1997; **95**: 2162 - 2168
- 4) Shah D, Azhar M, Oakley CM, Cleland JG, Nihoyannopoulos P: Natural history of secundum atrial septal defect in adults after medical or surgical treatment: A historical prospective study. *Br Heart J* 1994; **71**: 224 - 228
- 5) Reddy SC, Rao PS, Ewenko J, Kosciak R, Wilson AD: Echocardiographic predictors of success of catheter closure of atrial septal defect with the buttoned device. *Am Heart J* 1995; **129**: 76 - 82
- 6) Pepi M, Tamborini G, Pontone GL, Andreini D, Berna G, De Vita S, Maltagliati A: Initial experience with a new on-line transthoracic three-dimensional technique: Assessment of feasibility and of diagnostic potential. *Ital Heart J* 2003; **4**: 544 - 550
- 7) Morimoto K, Matsuzaki M, Tohma Y, Ono S, Tanaka N, Michishige H, Murata K, Anno Y, Kusukawa R: Diagnosis and quantitative evaluation of secundum-type atrial septal defect by transesophageal Doppler echocardiography. *Am J Cardiol* 1990; **66**: 85 - 91
- 8) Maeno YV, Benson LN, McLaughlin PR, Boutin C: Dynamic morphology of the secundum atrial septal defect evaluated by three dimensional transesophageal echocardiography. *Heart* 2000; **83**: 673 - 677
- 9) Bland JM, Altman DG: Statistical methods for assessing agreement between two methods of clinical measurement. *Lancet* 1986; **307**: 307 - 310
- 10) Faletra F, Scarpini S, Moreo A, Ciliberto GR, Austoni P, Donatelli F, Gordini V: Color Doppler echocardiographic assessment of atrial septal defect size: Correlation with surgical measurements. *J Am Soc Echocardiogr* 1991; **4**: 429 - 434
- 11) Zhuang L, Wang XF, Xie MX, Chen LX, Fei HW, Yang Y, Wang J, Huang RQ, Chen OD, Wang LY: Experimental study of quantitative assessment of left ventricular mass with contrast enhanced real-time three-dimensional echocardiography. *J Cardiol* 2004; **43**: 23 - 29
- 12) Xie MX, Wang XF, Cheng TO, Wang J, Lu Q: Comparison of accuracy of mitral valve area in mitral stenosis by real-time, three-dimensional echocardiography versus two-dimensional echocardiography versus Doppler pressure half-time. *Am J Cardiol* 2005; **95**: 1496 - 1499
- 13) Cheng TO, Xie MX, Wang XF, Wang Y, Lu Q: Real-time 3-dimensional echocardiography in assessing atrial and ventricular septal defects: An echocardiographic-surgical correlative study. *Am Heart J* 2004; **148**: 1091 - 1095
- 14) Wang XF, Deng YB, Nanda NC, Deng J, Miller AP, Xie MX: Live three-dimensional echocardiography: Imaging principles and clinical application. *Echocardiography* 2003; **20**: 593 - 604
- 15) Arore R, Jolly N, Kalra GS, Khalilullah M: Atrial septal defect after balloon mitral valvuloplasty: A transesophageal echocardiographic study. *Angiology* 1993; **44**: 217 - 221
- 16) Franke A, Kuhl HP, Rulands D, Jansen C, Erena C, Grabitz RG, Dabritz S, Messmer BJ, Flachskampf FA, Hanrath P: Quantitative analysis of the morphology of secundum-type atrial septal defects and their dynamic change using transesophageal three-dimensional echocardiography. *Circulation* 1997; **96**(9 Suppl): 323 - 327
- 17) Sideris EB, Sideris SE, Fowlkes JP, Ehly RL, Smith JE, Gulde RE: Transvenous atrial septal defect occlusion in piglets using a 'buttoned' double-disc device. *Circulation* 1990; **81**: 312 - 318
- 18) Ishii M, Kato H, Inoue O, Takagi J, Maeno Y, Sugimura T, Miyake T, Kumate M, Kosuga K, Ohishi K: Biplane transesophageal echo-Doppler studies of atrial septal defects: Quantitative evaluation and monitoring for transcatheter

- closure. *Am Heart J* 1993; **125**: 1363 - 1368
- 19) Thanopoulos BD, Laskari CV, Tsaousis GS, Zarayelyan A, Vekiou A, Papadopoulos GS: Closure of atrial septal defects with the Amplatzer occlusion device: Preliminary results. *J Am Coll Cardiol* 1998; **31**: 1110 - 1116
- 20) Sinha A, Nanda NC, Misra V, Khanna D, Dod HS, Vengala S, Mehmood F, Singh V: Live three-dimensional transthoracic echocardiographic assessment of transcatheter closure of atrial septal defect and patent foramen ovale. *Echocardiography* 2004; **21**: 749 - 753
- 21) Rosenfeld HM, van der Velde ME, Sanders SP, Colan SD, Parness IA, Lock JE, Spevak PJ: Echocardiographic predictors to candidacy for successful transcatheter atrial septal defect closure. *Cathet Cardiovasc Diagn* 1995; **34**: 29 - 34
- 22) Dall 'Agata A, McGhie J, Taams MA, Cromme-Dijkhuis AH, Spitaels SE, Breburda CS, Roelandt JR, Rogers AJ: Secundum atrial septal defect is a dynamic three-dimensional entity. *Am Heart J* 1999; **137**: 1075 - 1081

4 Relationships between live three-dimensional echocardiographic and intraoperative measurements of the defect area measured in 31 patients Upper : Linear regression of atrial septal defect area measured at the peak of P-wave by live three-dimensional echocardiography versus intraoperative method. Lower : Bland-Altman graph showing differences in each pair of measurements of the defect area obtained with the two methods. L3DE $\hat{=}$ live three-dimensional echocardiography. Other abbreviation as in Fig. 3. There was an excellent correlation between the measurements by L3DE at the peak of P-wave and Three-dimensional echocardiographic assessment of atrial septal defects. Article. Full-text available. $\hat{=}$ Three-dimensional echocardiography offers new insights into valvar function in atrioventricular septal defects (AVSDs). The aim of this study was to identify a morphological marker to predict the functional outcomes of left atrioventricular valves (AVVs) following the repair of AVSDs. Twenty-nine consecutive patients were evaluated preoperatively using 2-dimensional and 3-dimensional echocardiography. $\hat{=}$ Measurement of valve area by the trace method was difficult. Transesophageal echocardiography (TEE) showed a septum-like structure extending from the ventricular septum in the subvalvular area.